Biogeochemical simulation of microbially induced calcite precipitation with *Pararhodobacter* sp. strain SO1

Masaru Akiyama,*[,a] Satoru Kawasaki[b]

[a] Geoscience Research Laboratory Co., Ltd., JM Bldg. 4F, 3-1-6 Yamatohigashi, Yamato, Kanagawa, 242-0017, Japan

[b] Faculty of Engineering, Hokkaido University, Kita 13, Nishi 8, Kita-ku, Sapporo, Hokkaido 060-8628, Japan

*: Corresponding author

Geoscience Research Laboratory Co., Ltd., JM Bldg. 4F, 3-1-6 Yamatohigashi, Yamato, Kanagawa, 242-0017, Japan

Tel.: +81-46-200-2281

Fax: +81-46-200-2282

Email: akiyama@geolab.jp

ABSTRACT

Biogrouting is a ground improvement technique, which utilizes microorganisms. The numerical simulation of biogrouting is important to ensure efficient operation and to assess the applicability to the target ground. In this study, we compared syringe-scale biogrouting with biogeochemical simulation. Parameters suitable for practical applications were included. The rate constant and half-saturation constant of the reaction rate law in ureolytic bacteria *Pararhodobacter* sp. strain SO1, obtained from the simulation based on the urease activity test, were 1×10^{-8} mol/mg/s and 0.635 M, respectively. To achieve the same mineral precipitation in measurement and simulation, a setting in which only the calcite precipitated was used. In the sequential simulation of the solidification test, a variation in discharged Ca^{2+} concentration was reproduced by introducing an "adjustment index," which considers the microbial biomass contributing to the reaction. Moreover, for the re-injection test, in which microbes were injected again to further improve the biogrout strength, the settings were validated by the sequential simulation followed by predictive simulation on different injection dates. The results indicate that by conducting a biogeochemical simulation of calcite precipitation for biogrouting using ureolytic bacteria, the strength of biogrout can be predicted and managed.

KEYWORDS

biocementation, biogeochemical simulation, microbially induced calcite precipitation, numerical analysis, ureolytic bacteria

1. INTRODUCTION

In the field of geotechnical engineering, which integrates the knowledge and techniques of engineering, biology, and geology, a soil-improvement technique utilizing microbially induced calcite precipitation (MICP), known as biogrouting, has gained attention (e.g. [16, 18]). In the past 10 years, the development and application of this technique has greatly advanced [2, 6, 8, 14, 15, 18, 32]. Compared with conventional techniques based on chemical reactions, biogrouting exhibits a delayed effect; it solidifies after the grout solution has dispersed on the ground, allowing for materials such as fertilizer components to be used as solidifiers. Unlike concrete and glass-type materials, these components are less costly and have little environmental impact [17]. The basic reactions involved in this technique are the formation of HCO_3^- generated by the decomposition of urea and precipitation of calcite from the bond with Ca^{2+} [30]. Because ureolytic bacteria are present throughout soil, they can be isolated from the ground of interest and proliferated before use to contribute to the microbial ecosystem in the ground [6].

However, there are two major problems to be solved in actual implementation of soil improvement

technology by biogrouting: Verifying the applicability of biogrouting to the target ground and the cost of the assessment of microbial impact. Even if microbial reactions can be reproduced under controlled environmental conditions in a laboratory, it is difficult to reproduce and apply the results directly on the natural ground, where many additional factors must be considered in the gaseous, liquid, and solid phases. Microbial influence assessments, which are carried out using underground environment-related techniques, not only require temporal and long-term investigations, such as a boring survey of the progress of reactions in the ground and water quality measurement using a sampling well, but also involves high cost, labor, and environmental factors related to the difficulty of below-ground access [33].

An effective tool for overcoming such challenges is a biogeochemical simulation that enables inference of environmental factors affecting the area under investigation. The use of the simulator in implementing biogrout enables an estimation of how the microbial reactions alter ground strength, enabling the development of an appropriate implementation plan and efficient biogrout management while minimizing resources and labor. Studies establishing numerical models of biogrouting have been reported, which produce accurate mathematical descriptions of MICP and benefit further research and development [3, 10, 31]. Numerous issues related to biogrouting use under diverse eco-environmental conditions have been overcome [9]; we are close to the implementation of a simulation that is versatile and sufficiently accurate to be used in real-life scenarios.

Our aim was to construct a practical process of biogeochemical simulation of biogrouting and to extract problems to improve accuracy. In this study, while acquiring consistency between the measured and analytical values of biogrouting, analysis parameters necessary for practical application were acquired and parameter fitting of those was performed.

2. Biogeochemical simulation

Attempts to model underground microbial reactions have been carried out, particularly in studies of the geological disposal of radioactive waste, since the 1980s, when both the necessity and efficiency of using underground space increased (e.g. [13]). Many researchers have included the kinetic response of microbes in models based on chemical reaction simulations, which have been disseminated in many formats, both paid and free ([4], [25]). One such biogeochemistry simulator is The Geochemist's Workbench® Ver. 10.0 (Aqueous Solutions LLC., Champaign, IL, USA) (GWB) [4], which is equipped with suitable functions for biogrouting simulation. This program can extend the simulation to a two-dimensional model and features a thermodynamics database of organic substances, including urea as a standard function.

The fundamental reaction rate law for the microbial reaction in GWB is as shown in equation (1).

$$r = n_w k_+ [X] [m_D/(m_D + K'_D)] [m_A/(m_A + K'_A)] F_T \quad (1)$$

Here, r is reaction rate (mol/s), n_w is water content (kg), K_+ is reaction rate constant (mol/mg/s), [X] is biomass (mg/kg), m_D and m_A are the concentrations of electron donor and acceptor, K'_{D} and K'_{A} are half saturation constants, and F_{T} is the thermodynamic potential factor. F_{T} is defined the following equation (2).

$$F_{\mathrm{T}} = 1 - \exp[(\Delta G_r + m\Delta G_P)/\chi RT_K] \quad (2)$$

Here, ΔG_r is the free energy change of the microbial reaction (kJ/mol), m is the number of ATPs produced, ΔG_P is the free energy change of ATP synthesis (kJ/mol), χ is the average stoichiometric number (the number of times the rate determining step occurs), R is the gas constant (J/mol/K), and T_K is absolute temperature (K). The F_{T} term plays a role of regulating the reaction rate by thermodynamic constraints of the reaction field.

3. Syringe-scale biogrouting

3.1. Materials and Methods

3.1.1. Evaluation of urease activity

As a basic reference material for calculating the reaction rate constant, the ureolysis rate was

determined based on variations in the concentration of NH_4^+ produced during ureolysis by urease, and urease activity was evaluated. First, the ureolytic bacteria *Pararhodobacter* sp. strain SO1 (SO1) isolated from a beach rock in Okinawa [6] was inoculated into solid ZoBell 2216E medium [6] and cultured for over 72 h at 30°C. The cultured SO1 (1.0 g) was added to 100 mL of liquid ZoBell 2216E medium and cultured (with shaking at 160 rpm) for 48 h at 30°C. The number of bacteria in the culture solution was measured by determining the absorbance at a wavelength of 600 nm (OD_{600}). A 0.3 M urea solution containing 0.04% cresol red using a Tris-hydrochloric acid buffer solution (pH 8.0) was prepared as a solvent. The bacterial culture (1 mL) was added to 100 mL of the urea solution and agitated at 25°C to start the ureolytic reaction. After 5, 10, and 15 min, the urea solution (10 mL) was sterilized with a Minisart 16555K 0.2-μm membrane filter (Sartorius Stedim Japan Co., Ltd., Tokyo, Japan). To stop the ureolytic reaction, a strongly alkaline 10 M NaOH solution (0.1 mL) was added to denature and inactivate the urease; the NH_4^+ ion concentration was measured using a Handy Ammonia Meter TiN-9001 (Tokyo Chemical Laboratories Co. Ltd., Tokyo, Japan) and the enzyme activity as the substrate per unit of urease contained in the SO1 was calculated (in units of U = μmol/min).

3.1.2. Sand solidification

Using a cementation solution containing SO1, urea, and Ca^{2+}, a syringe-scale biogrouting as

described by Danjo and Kawasaki [6] was carried out. Briefly, 30-mL plastic syringe SS-30ESZ (Terumo Corporation, Tokyo, Japan) was attached to a 45-cm silicone tube. Sterilized coral sand (mean particle size (D_{50}), 0.7 mm, density, 2.74 g/cm^3) [6] was added to the syringe. SO1 culture solutions pre-cultured with liquid ZoBell 2216E medium (culture solutions of 0.01, 0.1, and 1.0 g biomass/100 mL) were injected in the syringe. After 30 min, the cementation solution shown in Table 1 was injected and incubated at 30°C. Simultaneous injection and discharge were carried out once per day for 15 days. After 3, 6, 9, and 12 days, Ca^{2+} in the effluent was measured using the Compact Calcium Ion Meter LAQUAtwin B-751 (Horiba Ltd., Kyoto, Japan). Fifteen days later, a needle penetration test was conducted on the solidified specimen using a Soft Rock Penetrometer SH-70 (maximum diameter of 40 mm; length of 285 mm; weight of 700 g) (Maruto Testing Machine Company, Tokyo, Japan) and unconfined compressive strength (UCS) was estimated using equation (3) below [6] according to the manufacturer's protocol. Here, *A* and *B* represent the needle penetration gradient and estimated UCS, respectively.

$$\log_{10} B = 0.978 \log_{10} A + 2.621 \qquad (3)$$

3.2. Results and discussion

To estimate the microbial biomass in solution, the turbidity at OD_{600} was measured. The OD_{600} of

the culture solution with SO1 was 1.192. According to Shimazaki [27], the relationship between the turbidity value measured with SO1 and the viable count (limited range, 1×10^{-7} to 1×10^{-10} cells/mL) was expressed using equation (4):

$$D = 0.1306 \ln C - 2.061 \quad (4)$$

where C and D represent the viable count and turbidity, respectively. The estimated microbial biomass in the culture solution used in the urease activity test, according to the equation (2) above, was 6.62×10^{10} cells/mL.

Figure 1 shows the results of the urease activity test. The plot of NH_4^+ concentration under the conditions of this study was linear and approximately followed equation (5):

$$F = 1.15 E - 3.699 \quad (5)$$

In this equation, E and F respectively represent the reaction time (minutes) and NH_4^+ concentration (ppm). According to our actual measurement, the NH_4^+ concentration after 15 min was 20.21 ppm; however, when the concentration was estimated using the approximation equation (5), which is based on the coordinates of four points, a value of 20.949 ppm compared with an initial

value of 3.699 ppm was obtained. Thus, for each mole of urea substrate, two moles of NH_4^+ were produced; because of the increase in NH_4^+ after 15 min of the reaction, the concentration of decomposed urea was 8.625 ppm. The concentration was converted into molarity units and the change in concentration per unit time (minutes) was calculated, revealing an enzyme activity of 3.19 U. In sensitivity simulation (described in the next section), the obtained numbers were used to determine a set of parameters.

Figure 2 shows the Ca^{2+} concentration in the effluent determined in the syringe-scale biogrouting conducted by sampling once every 3 days, and the estimated UCS 14 days after the start of the test. At 0.5 M urea, the Ca^{2+} concentration increased after 6 days following the addition of 0.01 g of SO1 and after 9 days with 0.1 g SO1. Additionally, the solution containing 0.4 M urea showed an increasing trend over time, although at a lower value than that observed for 0.5 M urea; the solution containing 0.3 M urea also increased slightly after 12 days. For any volume of SO1 added, increasing the urea and Ca^{2+} concentrations resulted in higher unconfined compressive strength. The highest strength of 4.3 MPa was observed when 1.0 g of SO1, 0.5 M urea, and 0.5 M Ca^{2+} were added. In presence of 0.3 and 0.4 M of urea and Ca^{2+}, however, varying volumes of SO1 did not greatly affect the strength.

The above results indicate a relationship between the concentrations of urea and Ca^{2+} in the injected cementation solution and Ca^{2+} concentration of the effluent. The relationship with the

unconfined compressive strength, however, required more detailed simulation. Thus, we focused on reproducing a microbial mineral precipitation reaction numerically, and thereafter matched the measured and analytical values of Ca^{2+} concentration variation in the effluent.

4. Simulation of sand solidification

4.1. Preparation for simulation

4.1.1. Sensitivity simulation for reaction rate

The initial solution in GWB based on the solution composition in the urease activity test (urea 0.3 M, NH_4^+ 3.699 ppm, 1×10^{-10} M Na^+, 1×10^{-4} M HCO_3^-, 1×10^{-4} M Cl^-, and pH 8.0) was set. If the charge balance of the solution changes drastically during simulation, the convergent calculation may diverge. By adding Na^+ and Cl^- (which are not directly associated with the settings of the reaction system) to the initial solution, this issue was avoided. GWB autonomously adjusts the charge balance. Moreover, because the chemical species, CO_2 (g) and NH_3 (aq), were restricted in the microbial reaction, they only appear in the system when released from the microbes involved in the reaction, the corresponding basic species (HCO_3^- and NH_4^+, respectively) were added to the initial solution in advance. For NH_4^+, a concentration of 3.699 ppm was measured at the beginning of the urease activity test. Because this concentration likely originated from the microbial culture solution, the same concentration parameters were applied to the initial solution to match the analytical value

with the measured value. Although Na^+, Cl^-, and HCO_3^- were not present in the solution, a minute volume (1×10^{-10} M) was input for calculation convergence improvement as a number corresponding to 0 M [34]. Because the reaction rate constant of biogrouting (which uses a ureolytic reaction) has been reported to range between 9.60×10^{-12} and 3.05×10^{-7} mol/mg/s (Table 2, [11, 20-22, 28-30, 32]), in this simulation, seven levels between 1×10^{-13} and 1×10^{-7} mol/mg/s were initially set to carry out the sensitivity test for the reaction rate constant. Because the half-saturation constant of urea has been reported to range from 3.21×10^{-3} to 0.305 M, five half-saturation constants between 1×10^{-4} and 1 M were set. In total, the sensitivity test was conducted for 35 cases and the parameters were precisely adjusted to match the results with the measured value.

To adopt the initial biomass estimated in the urease activity test (6.62×10^{10} cells/mL), as the initial biomass in the simulation, it was necessary to convert this value to the unit system of GWB (mg/kg). By setting the weights of a single microbe cell and 1 L of solvent to 9.5×10^{-13} mg [24] and 1 kg respectively, the initial biomass was converted to 623.0 mg/kg. Both parameters related to microbial propagation (growth yield and decay constant) were set to 1×10^{-10} [34] and polypeptone and yeast extract (two components involved in propagation) were removed from the initial solution.

In the ureolysis reaction, which is the main process involved in biogrouting, two moles of NH_3 and one mole of CO_2 are produced for each mole of urea decomposed (equations (6) and (7)) [12].

$$(NH_2)_2CO + H_2O \rightarrow H_2NCOO^- + NH_4^{++} \quad (6)$$

$$H_2NCOO^- + H2O \rightarrow HCO_3^- + NH_3 \quad (7)$$

In the thermodynamics database of GWB, urea is defined as a secondary chemical species. Thus, if the database is used with the default condition, urea is decomposed into NH_3 and CO_2 as soon as the simulation starts, based on the equilibrium reaction. To switch the hydrolysis of urea from an equilibrium reaction to a microbial kinetic response, the thermodynamics database was edited to consider urea as a redox species. As a result, urea and NH_4^+ form a redox pair. By breaking this pair using a “decouple” function during the simulation, it is possible to calculate the kinetic response. Additionally, in the kinetic simulation of microbes on GWB, the F_T term was set to consider thermodynamic equilibrium [5]. However, to make the hydrolysis of urea depend only on the microbial decomposition reaction, setting of the F_T term was disabled and the hydrolysis reaction of urea was described using the Monod equation [23], with urea concentration as the only basic structure in the reaction. Considering that calcite precipitated in biogrouting with ureolytic bacteria [1, 19], simulation with a setting in which only the calcite precipitated was conducted. Additionally, an actual urea reaction solution may contain residual nutrient broth present in the microbial culture solution, but because ureolysis is an enzymatic reaction that has been shown to progress even in media without nutrient broth, we did not take nutrient broth into account in these analyses.

4.1.2. Parameter settings

A simulation of a syringe-scale biogrouting was conducted based on the method of Danjo and Kawasaki [6]. Shimazaki [27] developed a regression equation that derives UCS from the calcium precipitation rate. However, because it is not possible to calculate UCS directly using GWB, we focused on the concentration of Ca^{2+} in the effluent to calculate the calcium precipitation rate with the above-mentioned regression equation. The concentration of Ca^{2+} in the effluent indicates the amount of Ca^{2+} in the injected cementation solution that was not utilized in solidification. Therefore, by measuring the Ca^{2+} concentration in the effluent, it is possible to indirectly determine the volume of calcite that precipitated out and estimate UCS using the regression equation. Based on these findings, from the simulation of GWB in this study, the effluent Ca^{2+} concentration left unused in calcite precipitation was used as an index to match the measured value with the simulated value.

Using the reaction rate constant and half-saturation constant obtained as described in the previous paragraph, a 15-day-long reproducibility simulation was carried out. For the simulation, a culture solution containing 0.01, 0.1, and 1.0 g (estimated living microbes were 6.0×10^8, 2.0×10^9, and 6.0×10^9 cell/mL, respectively) of SO1 (in parenthesis are the estimated viable counts at the time of use) was used, as well as a cementation solution with urea and calcium chloride concentrations of 0.3, 0.4, and 0.5 M added. To reproduce the design of the syringe-scale biogrouting in the simulation, a

cementation solution with the same composition as that described in Table 1, was used as the initial solution and the kinetic response of the microbes was set to 1 day. In this chapter, sequential simulation was carried out, in which the volume of calcite that precipitated on the first day was assumed to act as the second day's initial condition, and the cementation solution of the second day had the same composition as that of the first day. Using this method, it was possible to represent the injection of cementation solution, accumulation of calcite, and variation of Ca^{2+} concentration in the effluent once per day. However, using this method, the calcite volume was expected to increase linearly; that is, the concentration of Ca^{2+} in the effluent was likely to remain constant. Hence, to match the trend of the simulation to that of the measurement, in which the Ca^{2+} concentration increases over time, a coefficient to adjust the reaction rate was derived.

4.1.3. Introduction of "adjustment index"

Among the parameters used to calculate the reaction rate, the rate constant and half-saturation constant are unique numerical values representing the characteristics of the SO1 being analyzed, and therefore, it was desirable that they remained constant throughout the study. A possible explanation for the increased concentration of discharged Ca^{2+} over time during the measurement is that the cells of SO1 in the syringe after injection were covered by precipitated calcite, resulting in a lower volume of SO1, contributing to the solidification [7]. Based on this assumption, we focused on the

1 microbial biomass in the sequential simulation and adjusted the value to match that of the actual
2 phenomenon.
3 From the Ca^{2+} concentration measured in the effluent, it is possible to calculate the volume of
4 calcite precipitated for one day of injection, as well as the integrated volume of precipitated calcite
5 until injection. Because the volumes of the syringe and sand particles used in the experiment were
6 constant throughout the simulation with repeated injection/discharge, we inferred that the maximum
7 precipitation volume of calcite in a test with the same microbial biomass approximates to a constant
8 value regardless of the cementation solution concentration. In agreement with the hypothesis that the
9 microbes gradually lose contact with the reaction solution because of the calcite precipitation, the
10 microbial biomass that contributes to calcite precipitation on the day of injection may depend on the
11 volume of calcite precipitated until the preceding day. Therefore, we estimated the microbial
12 biomass on the day of injection using equation (8) below:
13
14 $$y = y_0 \left[1 - (x/x_{max})^n\right] \qquad (8)$$
15
16 The variable x in the above equation is the integrated volume of calcite precipitated until the
17 previous day (g), x_{max} is the maximum volume of precipitated calcite when an arbitrary microbial
18 biomass is added (g), y_0 is the initial biomass (g), y is the microbial biomass present in the reaction

1 that contributes to the precipitation of calcite (g), and *n* is named the “adjustment index”. In the
2 sequential simulation of this study, the adjustment index can contribute to taking over the biomass
3 between sequential reactions because the relationship between biomass and metabolism is
4 mathematically presented through allometry (e.g. [4], [25], [26]). All measured values, including
5 interpolated values, were compared with the simulated values using arbitrary *n* and x_{max} and the
6 square sum of errors was calculated at all comparison points. Using this procedure, we defined the
7 combination of *n* and x_{max} that minimized the square sum of errors. However, for practical
8 convenience, we set *n* as the same value regardless of the microbial biomass and determined x_{max}
9 with the respective microbial biomass at each moment. The simulation using these *n* and x_{max} values
10 was carried out to determine the microbial biomass on each day using sequential calculations.
11
12 *4.2. Results and discussion*
13 *4.2.1. Determination of parameters and settings of simulation*
14 Because the NH_4^+ concentration, measured before the start of the reaction, is thought to be a
15 product of the added SO1 culture solution, the NH_4^+ concentration of the initial solution to 3.699
16 ppm was set in the simulation to match the measured value. The target value (obtained after 15 min
17 of the reaction) was set to 20.95 ppm and a sensitivity test was conducted.
18 Table 3 shows the simulation results of 35 cases performed with the initial biomass above and

classified by the reaction rate constant. With the same reaction rate constant, the NH_4^+ concentration after 15 min generally decreased as the half-saturation constant increased. The cases with concentration the closest to the target value after 15 min were No. 29 and 30, with a reaction rate constant of 1×10^{-8} mol/mg/s. The NH_4^+ concentrations in these cases after 15 min were respectively 44.06 and 16.11 ppm. Therefore, we fine-tuned the parameter and set the half-saturation constant to 0.1–1 M to approximate this value to the target value after 15 min. Case No. 36, which showed an NH_4^+ concentration of 20.94 ppm after 15 min, showed a half-saturation constant of 0.635 M. Based on the results above, the reaction rate constant of 1×10^{-8} mol/mg/s and half-saturation constant of 0.635 M as microbial parameters were adopted for this simulation.

4.2.2. Adjustment index and simulation of sand solidification

Based on the sensitivity test, for the microbial biomass adjustment used in sequential simulation and by setting the adjustment index *n* to 3.2, the maximum precipitation amount of calcite was 6.26 M with a microbial addition of 1.0 g, 5.58 M with addition of 0.1 g, and 4.85 M with 0.01 g microbes when the square sum of errors of the measured and theoretical values were at a minimum (Table 4). Figure 3 shows the relationship between the integrated amount of calcite that precipitated until the previous day and precipitable amount of calcite, as well as the graph of the measured value.

The results of the simulation were obtained with an adjustment index $n = 3.2$, and the respective

microbial biomasses are shown in Figure 4 (a)–(c). From the Ca^{2+} concentration with the maximum microbial addition (1.0 g), the simulation values showed approximately the same change over time as the measured values. However, when 0.1 or 0.01 g was added, the Ca^{2+} concentration remained relatively constant over the test period. This indicates that even if the maximum urease activity had been achieved and calcite precipitation had occurred with the microbial biomass set in the simulation, the precipitation volume would not be sufficiently large to suppress the microbial reaction on the next day, suggesting that the microbial biomass setting was too small. To increase the reaction rates with the addition of 0.1 and 0.01 g, we adjusted the parameters suitably to increase microbial biomass.

In each case, we gradually increased the microbial biomass by 10 mg/kg to obtain the initial biomass that minimized the square sum of errors of the measured value and simulation value of the discharged Ca^{2+} concentration. With these adjustments, we increased the biomass from 570 to 3,420 mg/kg in the case of 0.01 g and from 1,900 to 4,370 mg/kg in the case of 0.1 g; additionally, the square sum of errors was minimized. The results of sequential simulation to adjust the microbial biomass are shown in Figure 5 (a)–(c). After adjusting for the microbial biomass, Ca^{2+} consumption in the initial stage of simulation was boosted, and the concentration of discharged Ca^{2+} increased over time in the simulation. The measured and simulated values also showed a high correlation, with consistency between the two showing great improvement (Fig. 6).

The initial biomass required adjustment for the following possible reasons: SO1 continued to propagate or decay after injection, inactivated urease or biomass was present, the cells were detached from the surface of the sand, and precipitated calcite stimulated even further precipitation as a seed crystal. To understand the mechanism of action leading to microbial biomass adjustment, it is necessary to conduct separate tests specialized for microbial biomass measurement such as chronological change in the distribution and established number of microbes, not only in the effluent but also in the specimen, as well as the relationship of these factors with the solution concentration. Moreover, in the urease activity test and syringe-scale biogrouting, the presence or absence of nutrient broth may have affected the propagation and reaction rate of SO1. Therefore, it is necessary to more accurately verify the urease activity of SO1 and establish standards for the properties of ureolytic bacteria that can be used in biogrouting, including SO1. Overall, our result suggests that by conducting a preliminary solidification test and simulation for a specimen of collected ground material, with multiple levels of microbial addition it is possible to predict the solidification reaction on the ground based on the microbial biomass before actual implementation.

5. Extended simulation to re-injection process

5.1. Materials and methods

In the syringe-scale biogrouting discussed in previous sections, the concentration of discharged

Ca^{2+} was increased after the 7th day from the start of injection. Thus, the microbial biomass that contributes to calcite precipitation began decreasing significantly while the volume of calcite precipitation per injection of cementation solution was reduced. Hence, a re-injection test was carried out consisting of another SO1 injection into the specimen during the solidification test to stimulate the precipitation of calcite. According to the method of the syringe-scale biogrouting, the injection and discharge of cementation solution were carried out once per day. Using a microbial addition of 1.0 g and urea concentration of 0.5 M, which were determined to be optimal conditions in the syringe-scale biogrouting described in the previous sections, the culture solution was re-injected 7 days after the start of the test. The effluent was sampled every day and its Ca^{2+} concentration was measured. After 14 days, the estimated UCS of the specimen was measured using a Soft Rock Penetrometer.

Using the simulation parameters obtained above, the re-injection test was reproducibly simulated. On day 7 of the simulation, the number of microbes contributing to calcite precipitation (H_1 mg/kg) was obtained as a numerical value. Because 5,700 mg/kg additional microbial biomass was added during re-injection, sequential simulation was resumed with a microbial biomass of H_1+5,700 mg/kg on day 7. To express the gradual decrease in microbial biomass contributing to calcite precipitation in the sequential calculation after re-injection (similar to that in the syringe-scale biogrouting), it is necessary to recalculate the maximum precipitation volume of calcite, x_{max}, which corresponds to the

injected microbial biomass. From the three steps of microbial biomass used in the syringe-scale biogrouting and corresponding values of x_{max}, the logarithmic approximation equation (equation (9)) was obtained as follows:

$$x_{max} = 0.6123 \ln(H) + 5.1919 \quad (9)$$

Variable b is the microbial biomass (×1000 mg/kg) and x_{max} is the maximum precipitated volume of calcite (M) when an arbitrary microbial biomass is added. Using this equation and the microbial biomass that contributes to calcite precipitation (retained from the first injection of sequential simulation), as well as the added microbial biomass (5,700 mg/kg), the total microbial biomass was calculated and x_{max} was determined, which was used in sequential calculation of the re-injection (Table 5). For the adjustment index, the same n =3.2 as used in the simulation was adopted.

In the re-injection test in the simulation, in addition to the case in which injection was conducted after 7 days as in the actual measurement, re-injection of biomass in other cases were carried out after 4 and 10 days. In these cases, the simulation period was extended to 15 days after re-injection.

5.2. Results and discussion

5.2.1. Estimated UCS and Ca^{2+} concentration in re-injection test

Figure 7 shows the variation in Ca^{2+} concentration in the effluent and estimated UCS in the re-injection test. Immediately after re-injection (after 7 days), a temporary increase in the concentration was observed, but the concentration decreased again starting on day 8 to a similar level similar as before re-injection. After that, the value remained nearly constant until day 14. The estimated UCS, after both the injection test and re-injection test, was higher than 10 MPa, which was more than 2-fold the strength of the specimen in a single injection test. These results indicate that the addition of SO1, through re-injection, effectively uses the Ca^{2+} added during the test period to precipitate calcium and, as a result, stimulates the strength of the specimen.

5.2.2. Reproducible and predictive simulation of re-injection test

Figure 8 shows the result of reproducible simulation of the re-injection test. The graph does not fully represent the high increase in Ca^{2+} concentration on the day of re-injection, but the trend was similar to that of the measured value in the remaining period, with a value of approximately 2.0 g/L or lower. Figure 9 and Table 6 summarize the results of the reproducible simulation in which we changed the re-injection dates to days 4 and 10. In their simulations, we observed a gradual increase in Ca^{2+} concentration from approximately day 15, reaching a peak after day 22. In all cases, the Ca^{2+} concentration after re-injection initially remained at approximately less than 1.0 g/L for a few days, began increasing at around 10 days after re-injection, and finally reached a maximum at 15 days

after re-injection. At 15 days after starting the simulation, a large increase in Ca^{2+} concentration in the effluent was observed only in the case of re-injection on day 4. When the volume of calcite precipitation was calculated, early re-injection tended to result in a higher precipitation volume. However, although the precipitation volume of cases injected on days 4 and 7 were nearly the same, it is necessary to consider that after 15 days, while the Ca^{2+} concentration of the day 4-injected case began increasing, the microbial biomass in the day 7-injected case still showed a considerably high potential for contributing to calcite precipitation, as well as a higher precipitation volume compared to day 10 injection. Therefore, it was analytically confirmed that re-injection after 7 days was the most appropriate date among the three dates tested.

Although re-injection was conducted only once during a test period of 15 days, even in cases in which it is necessary to analyze multiple-setting conditions based on multiple parameters, such as an increased number of injections, doubling the microbial biomass, or changing the simulation period with a numerical simulation, it is easy to derive the predicted result and validate the set conditions before actual implementation.

6. CONCLUSIONS

In this study, based on experimental results related to the development of biogrouting with ureolytic bacteria, we obtained the appropriate parameters for use in biogeochemical simulation, and

carried out a reproducible simulation with emphasis on adjusting the concentration of dischargedCa^{2+}. The following are the major findings of this study:

1) From the simulation of the urease activity test and sensitivity test, we obtained a reaction rate constant of 1×10^{-8} mol/mg/s and half-saturation constant of 0.635 M for ureolysis with *Pararhodobacter* sp. strain SO1 in this study.

2) By introducing an "adjustment index," which considers the variation in microbial biomass contributing to the reaction, into the sequential simulation of syringe-scale biogrouting, we reproduced the variation in the concentration of discharged Ca^{2+} with a microbial addition of 1.0 g.

3) We analytically reproduced a re-injection test aimed at improving the solidification strength and demonstrated its potential application in predictive simulation with different set conditions.

Based on these findings, by conducting a solidification test using ground material and biogeochemical simulation before actual construction, it is possible to predict the strength during

1 construction and optimize its management, which will contribute to reducing the use of resources
2 and labor in the entire construction. However, in cases other than the 1.0 g microbial addition, it is
3 necessary to adjust the initial microbial biomass. Additionally, a few other issues, such as the
4 difficulty in describing the consumption of microbes with nutrient broth, were raised. The diversity
5 of soil properties in the practical field should be considered as an important factor. Future studies are
6 needed to conduct verification simulation to clarify these issues and develop an efficient procedure
7 for adjusting the parameter set including the effects of soil properties.
8

REFERENCES

1. Achal V, Kawasaki S (2016) Biogrout: A novel binding material for soil improvement and concrete repair. Front Microbiol 7:314.
2. Akiyama M, Kawasaki S (2012) Microbially mediated sand solidification using calcium phosphate compounds. Eng Geol 137–138:29–39.
3. Barkouki T, Martinez BC, Mortensen BM, Weathers TS, DeJong JT, Ginn TR, Spycher NF, Smith RW, Fujita Y (2011) Forward and inverse bio-geochemical modeling of microbially induced calcite precipitation in half-meter column experiments. Transp Porous Med 90:23–39.
4. Bethke CM (2008) Geochemical and biogeochemical reaction modeling. Cambridge University Press, New York. https://doi.org/10.1017/CBO9780511619670
5. Bethke CM, Sanford RA, Kirk MF, Jin Q, Flynn TM (2011) The thermodynamic ladder in geomicrobiology. Amer J Sci 311:183–210.
6. Danjo T, Kawasaki S (2016) Microbially induced sand cementation method using *Pararhodobacter* sp. strain SO1, inspired by beachrock formation mechanism. Mater Trans 57: 428–437.
7. De Muynck W, De Belie N, Verstraete W (2010) Microbial carbonate precipitation in construction materials: A review. Ecol Eng 36:118–136.
8. DeJong JT, Fritzges MB, Nusslein K (2006) Microbial induced cementation to control sand

response to undrained shear. J Geotech Geoenviron Eng 132:1381–1392.

9. DeJong JT, Soga K, Kazazanjian E, Burns S, Van Paassen LA, Al Qabany A, Aydilek A, Bang SS, Burbank M, Caslake LF, Chen CY, Cheng X, Chu J, Ciurli S, Esnault-Filet A, Fauriel S, Hamdan N, Hata T, Inagaki Y, Jefferies S, Kuo M, Loloui L, Larrahondo J, Manning DAC, Martinez B, Montoya BM, Nelson DC, Palomino A, Renforth P, Santamarina JC, Seagren EA, Tanyu B, Tsesarsky M, Weaver T (2013) Biogeochemical processes and geotechnical applications: progress opportunities and challenges. Géotechnique 63:287–301.

10. Fauriel S, Laloui L (2012) A bio-chemo-hydro-mechanical model for microbially induced calcite precipitation in soils. Comp Geotech 46:104–120.

11. Fidaleo M, Lavecchia R (2003) Kinetic study of enzymatic urea hydrolysis in the pH range 4-9. Chem Biochem Eng Q 17:311–318.

12. Fujita M, Nakashima K, Achal V, Kawasaki S (2017) Whole'cell evaluation of urease activity of Pararhodobacter sp. isolated from peripheral beachrock. Biochem Eng J 124: 1–5.

13. Humphreys PN, West JM, Metcalfe R (2010) Microbial effects on repository performance. Quintessa QRS-1378Q-1, version 3.0.

14. Inagaki Y, Tsukamoto M, Mori H, Sasaki T, Soga K, Qabany AAl, Hata T (2011) The influence of injection conditions and soil types on soil improvement by microbial functions. Proc Geo-Front 4021–4030.

15. Ivanov V, Chu J (2008) Applications of microorganisms to geotechnical engineering for bioclogging and biocementation of soil in situ. Rev Environ Sci Biotech 7:139–153.

16. Jonkers HM, Van Loosdrecht KCM (2010) BioGeoCivil Engineering. Ecol Eng 36:97–98.

17. Kawasaki S, Murao A, Hiroyoshi N, Tsunekawa M, Kaneko K (2006) Fundamental study on novel grout cementing due to microbial metabolism. J Japan Soc Eng Geol 47:2–12 (in Japanese with English abstract).

18. Khodadadi TH, Kavazanjian E, Van Paassen L, Dejong J (2017) Bio-Grout Materials: A Review. Geotech Spe Pub (288 GSP), 1–12. DOI: 10.1061/9780784480793.001

19. Kim G, Youn H (2016) Microbially induced calcite precipitation employing environmental isolates. Materials (Basel) 9:468.

20. Lauchnor EG, Topp DM, Parker AE, Gerlach R (2015) Whole cell kinetics of ureolysis by *Sporosarcina pasteurii*. J Appl Microbiol 118:1321–1332.

21. Maclachlan E, El Mountassir G, Lunn RJ (2013) Use of bacterial ureolysis for improved gelation of silica sol in rock grouting. Géotech Lett 3:180–184.

22. Mahanty B, Kim S, Kim CG (2014) *Bacillus pasteurii* mediated ureolysis – a numerical approach for kinetic analysis. Int J Environ Eng 1:41–47.

23. Monod J (1949) The growth of bacterial cultures. Ann Rev Microbiol 3:371–394.

24. Neidhardt FC, Ingraham JL, Schaechter M (1990) Physiology of the bacterial cell: a molecular

approach. Sinauer Associates Inc., Sunderland, MA.

25. Parkhurst DL (1995) PHREEQC-A computer program for speciation, reaction-path, advective-transport, and inverse geochemical calculations. US Geol Surv Water Resour Invest Rep 95–4227.

26. Shestopaloff YK (2016) Metabolic allometric scaling model: combining cellular transportation and heat dissipation constraints. J Exp Biol 219:2481–2489.

27. Shimazaki S (2015) Experimental study on coral sand solidification test using *Pararhodobacter* sp. M.D. Thesis, Hokkaido Univ (in Japanese).

28. Tobler DJ, Cuthbert MO, Greswell RB, Riley MS, Renshaw JC, Handley-Sidhu S, Phoenix VR, (2011) Comparison of rates of ureolysis between *Sporosarcina pasteurii* and an indigenous groundwater community under conditions required to precipitate large volumes of calcite. Geochim Cosmochim Acta 75:3290–3301.

29. Tobler DJ, Cuthbert MO, Phoenix VR (2014) Transport of Sporosarcina pasteurii in sandstone and its significance for subsurface engineering technologies. Appl Geochem 42:38–44.

30. Van Paassen LA, Harkes MP, Van Zwieten GA, Van der Zon WH, Van der Star WRL, Van Loosdrecht MCM (2009) Scale up of BioGrout: a biological ground reinforcement method, Proc 17th Int Conf Soil Mech Geotech Eng 2328–2333.

31. Van Wijingaarden WK, Vermolen FJ, Van Meurs GAM, Vuik C (2011) Modelling biogrout: A

new ground improvement method based on microbial-induced carbonate precipitation. Transp Porous Med 87:397–420.

32. Whiffin VS, Van Paassen LA, Harkes MP (2007) Microbial carbonate precipitation as a soil improvement technique. Geomicrobiol J 24:417–423.

33. Wilkins MJ, Daly RA, Mouser PJ, Trexler R, Sharma S, Cole DR, Wrighton KC, Biddle JF, Denis EH, Fredrickson JK, Kieft TL, Onstott TC, Peterson L, Pfiffner SM, Phelps TJ, Schrenk MO (2014) Trends and future challenges in sampling the deep terrestrial biosphere. Front Microbiol 5:481.

34. Xu T, Sonnenthal E, Spycher N, Pruess K (2004) TOUGHREACT User's Guide: A simulation program for non-isothermal multiphase reactive geochemical transport in variably saturated geologic media. Earth Science Division, Lawrence Berkeley National Laboratory, University of California, LBNL-55460.

FIGURE CAPTIONS

Fig. 1. Variation in NH_4^+ concentration in urease activity test.

Fig. 2. Measured Ca^{2+} concentration in effluent of syringe-scale biogrouting (line graph) and estimated unconfined compressive strength (value next to the plot).

Fig. 3. Relationship between accumulated amount and precipitated amount of calcite corresponding to injected biomass. The plots of measured data include interpolated values.

Fig. 4. Simulation of syringe-scale biogrouting.

Fig. 5. Simulation of syringe-scale biogrouting (modification of initial biomass: 6.0 times of the original amount in the case of 0.01 g and 2.3-fold in the case of 0.1 g).

Fig. 6. Comparison between measured and simulated values of Ca^{2+} concentration in the effluent of syringe-scale biogrouting.

Fig. 7. Variation in Ca^{2+} concentration in the effluent of re-injection test (line graph) and estimated unconfined compressive strength (value next to the plot).

Fig. 8. Comparison between simulated and measured values of re-injection test.

Fig. 9. Influence of re-injection day on the variation in Ca^{2+} concentration.

Figure 1

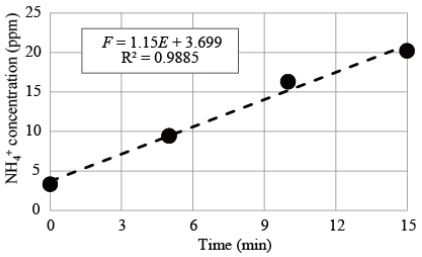
F = 1.15E + 3.699
R² = 0.9885
NH4+ concentration (ppm)
Time (min)
0
5
10
15
20
25
0
3
6
9
12
15

1

Figure 2

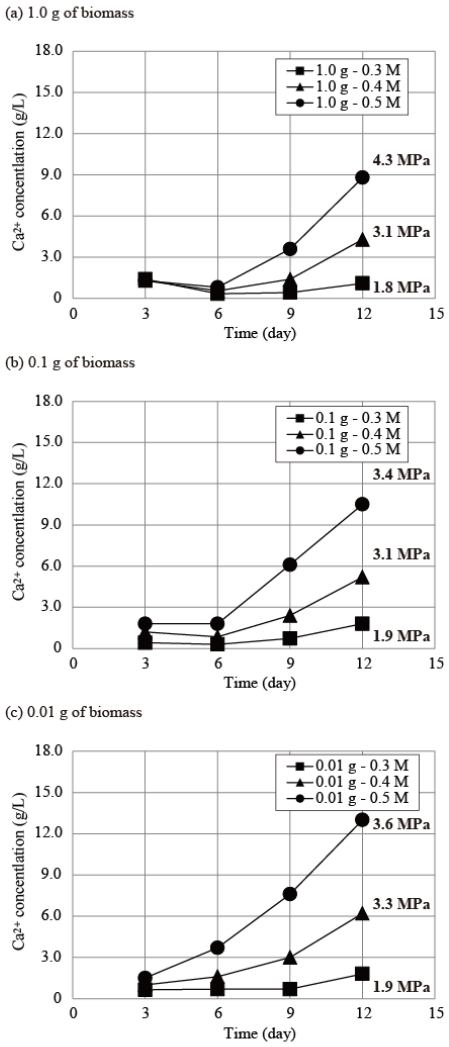
(a) 1.0 g of biomass
1.0 g - 0.3 M
1.0 g - 0.4 M
1.0 g - 0.5 M
4.3 MPa
3.1 MPa
1.8 MPa
Ca2+ concentlation (g/L)
Time (day)
(b) 0.1 g of biomass
0.1 g - 0.3 M
0.1 g - 0.4 M
0.1 g - 0.5 M
3.4 MPa
3.1 MPa
1.9 MPa
Ca2+ concentlation (g/L)
Time (day)
(c) 0.01 g of biomass
0.01 g - 0.3 M
0.01 g - 0.4 M
0.01 g - 0.5 M
3.6 MPa
3.3 MPa
1.9 MPa
Ca2+ concentlation (g/L)
Time (day)

Figure 3

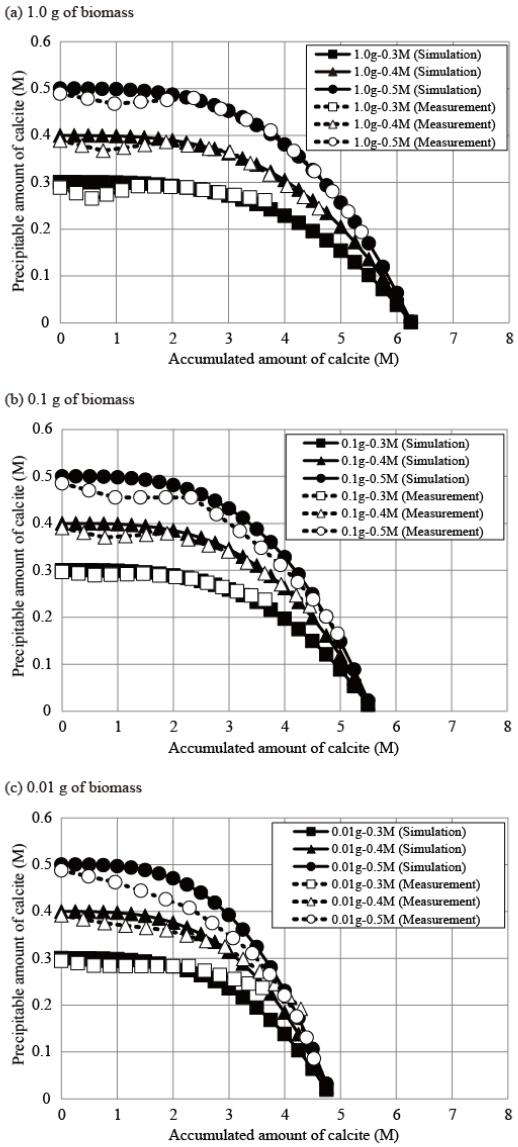
(a) 1.0 g of biomass
1.0g-0.3M (Simulation)
1.0g-0.4M (Simulation)
1.0g-0.5M (Simulation)
1.0g-0.3M (Measurement)
1.0g-0.4M (Measurement)
1.0g-0.5M (Measurement)
Precipitable amount of calcite (M)
Accumulated amount of calcite (M)
(b) 0.1 g of biomass
0.1g-0.3M (Simulation)
0.1g-0.4M (Simulation)
0.1g-0.5M (Simulation)
0.1g-0.3M (Measurement)
0.1g-0.4M (Measurement)
0.1g-0.5M (Measurement)
Precipitable amount of calcite (M)
Accumulated amount of calcite (M)
(c) 0.01 g of biomass
0.01g-0.3M (Simulation)
0.01g-0.4M (Simulation)
0.01g-0.5M (Simulation)
0.01g-0.3M (Measurement)
0.01g-0.4M (Measurement)
0.01g-0.5M (Measurement)
Precipitable amount of calcite (M)
Accumulated amount of calcite (M)

1

Figure 4

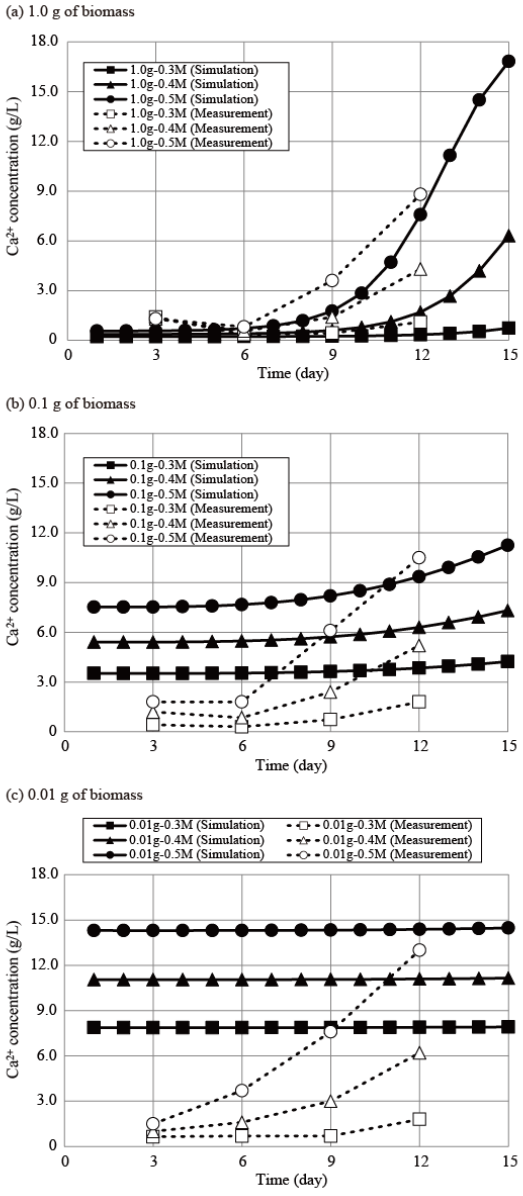
(a) 1.0 g of biomass
1.0g-0.3M (Simulation)
1.0g-0.4M (Simulation)
1.0g-0.5M (Simulation)
1.0g-0.3M (Measurement)
1.0g-0.4M (Measurement)
1.0g-0.5M (Measurement)
Ca2+ concentration (g/L)
Time (day)
(b) 0.1 g of biomass
0.1g-0.3M (Simulation)
0.1g-0.4M (Simulation)
0.1g-0.5M (Simulation)
0.1g-0.3M (Measurement)
0.1g-0.4M (Measurement)
0.1g-0.5M (Measurement)
Ca2+ concentration (g/L)
Time (day)
(c) 0.01 g of biomass
0.01g-0.3M (Simulation)
0.01g-0.4M (Simulation)
0.01g-0.5M (Simulation)
0.01g-0.3M (Measurement)
0.01g-0.4M (Measurement)
0.01g-0.5M (Measurement)
Ca2+ concentration (g/L)
Time (day)

1

Figure 5

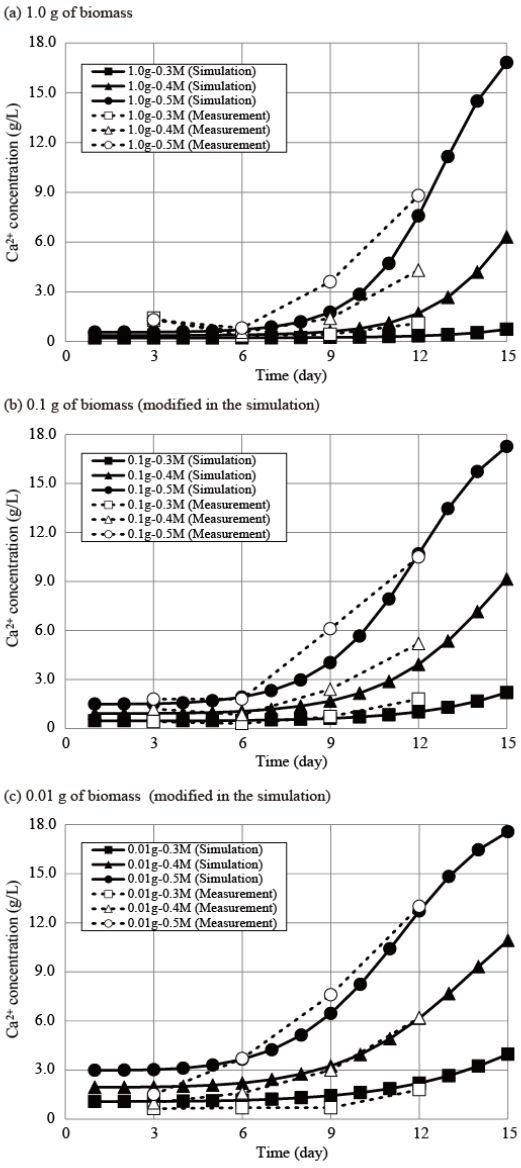
(a) 1.0 g of biomass
1.0g-0.3M (Simulation)
1.0g-0.4M (Simulation)
1.0g-0.5M (Simulation)
1.0g-0.3M (Measurement)
1.0g-0.4M (Measurement)
1.0g-0.5M (Measurement)
Ca2+ concentration (g/L)
Time (day)
(b) 0.1 g of biomass (modified in the simulation)
0.1g-0.3M (Simulation)
0.1g-0.4M (Simulation)
0.1g-0.5M (Simulation)
0.1g-0.3M (Measurement)
0.1g-0.4M (Measurement)
0.1g-0.5M (Measurement)
Ca2+ concentration (g/L)
Time (day)
(c) 0.01 g of biomass (modified in the simulation)
0.01g-0.3M (Simulation)
0.01g-0.4M (Simulation)
0.01g-0.5M (Simulation)
0.01g-0.3M (Measurement)
0.01g-0.4M (Measurement)
0.01g-0.5M (Measurement)
Ca2+ concentration (g/L)
Time (day)

1

Figure 6

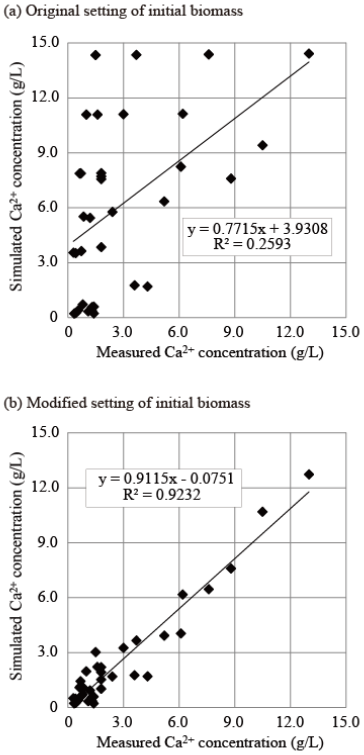
(a) Original setting of initial biomass
Simulated Ca^{2+} concentration (g/L)
Measured Ca^{2+} concentration (g/L)
y = 0.7715x + 3.9308
R² = 0.2593
0
3.0
6.0
9.0
12.0
15.0
(b) Modified setting of initial biomass
Simulated Ca^{2+} concentration (g/L)
Measured Ca^{2+} concentration (g/L)
y = 0.9115x - 0.0751
R² = 0.9232

1

Figure 7

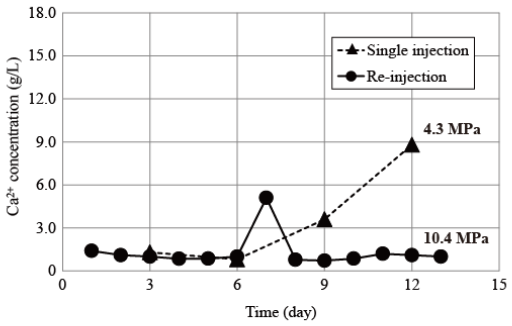
18.0
15.0
12.0
9.0
6.0
3.0
0
0
3
6
9
12
15
Ca2+ concentration (g/L)
Time (day)
Single injection
Re-injection
4.3 MPa
10.4 MPa

1

Figure 8

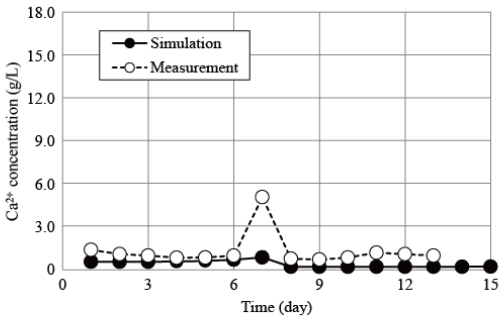
18.0
15.0
12.0
9.0
6.0
3.0
0
Ca2+ concentration (g/L)
Simulation
Measurement
0
3
6
9
12
15
Time (day)

1

Figure 9

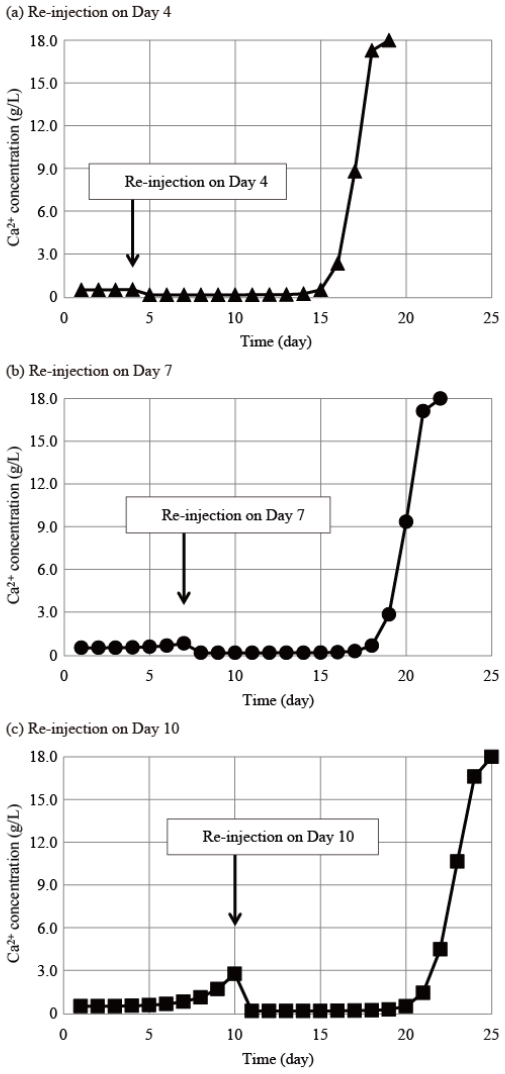
(a) Re-injection on Day 4
Re-injection on Day 4
Ca2+ concentration (g/L)
Time (day)
(b) Re-injection on Day 7
Re-injection on Day 7
Ca2+ concentration (g/L)
Time (day)
(c) Re-injection on Day 10
Re-injection on Day 10
Ca2+ concentration (g/L)
Time (day)

Table 1

Composition of cementation solution (solvent: artificial seawater).

Reagent	Case of 0.3M	Case of 0.4M	Case of 0.5M
Urea (M)	0.3	0.4	0.5
NH_4^+ (M)	0.187	0.187	0.187
Na^+ (M)	0.505	0.505	0.505
HCO_3^- (M)	0.028	0.028	0.028
Cl^- (M)	1.347	1.547	1.747
Ca^{2+} (M)	0.31	0.41	0.51
Mg^{2+} (M)	0.055	0.055	0.055
SO_4^{2-} (M)	0.029	0.029	0.029
K^+ (M)	0.01	0.01	0.01
nutrient broth (g/L)	3.0	3.0	3.0

pH =8.1

Table 2

Reaction rate constant and half saturation constant related to urease activity.

References	Rate constant (mol/mg/sec)	Half saturation constant (M)
Fidaleo and Lavecchia [11]	3.05×10^{-7}	3.21×10^{-3}
Whiffin [32]	2.00×10^{-7}	0.2
Van Paassen [30]	-	0.055
Tobler et al. [28]	1.15×10^{-11}	-
	6.32×10^{-10}	-
Maclachlan et al. [21]	8.33×10^{-10}	-
	2.22×10^{-9}	-
Tobler et al. [29]	1.92×10^{-8}	-
Mahanty et al. [22]	9.60×10^{-12}	-
	1.73×10^{-10}	-
Lauchnor et al. [20]	8.92×10^{-8}	0.305

Table 3

NH_4^+ concentration in sensitivity analysis after 15 days.

No.	Rate constant (mol/mg/sec)	Half saturation constant (M)	NH_4^+ concentration (mg/L)
1	1×10^{-13}	0.0001	3.70
2	1×10^{-13}	0.001	3.70
3	1×10^{-13}	0.01	3.70
4	1×10^{-13}	0.1	3.70
5	1×10^{-13}	1	3.70
6	1×10^{-12}	0.0001	3.70
7	1×10^{-12}	0.001	3.70
8	1×10^{-12}	0.01	3.70
9	1×10^{-12}	0.1	3.70
10	1×10^{-12}	1	3.70
11	1×10^{-11}	0.0001	3.75
12	1×10^{-11}	0.001	3.75
13	1×10^{-11}	0.01	3.75
14	1×10^{-11}	0.1	3.74
15	1×10^{-11}	1	3.71
16	1×10^{-10}	0.0001	4.24
17	1×10^{-10}	0.001	4.24
18	1×10^{-10}	0.01	4.22
19	1×10^{-10}	0.1	4.10
20	1×10^{-10}	1	3.82
21	1×10^{-9}	0.0001	9.09
22	1×10^{-9}	0.001	9.07
23	1×10^{-9}	0.01	8.92
24	1×10^{-9}	0.1	7.74
25	1×10^{-9}	1	4.95
26	1×10^{-8}	0.0001	57.60
27	1×10^{-8}	0.001	57.43
28	1×10^{-8}	0.01	55.86
29	1×10^{-8}	0.1	44.06
30	1×10^{-8}	1	16.11
31	1×10^{-7}	0.0001	556.23
32	1×10^{-7}	0.001	554.46
33	1×10^{-7}	0.01	537.44
34	1×10^{-7}	0.1	412.44
35	1×10^{-7}	1	127.79
36	1×10^{-8}	0.635	20.94

Table 4

Theoretical value of adjustment index and maximum accumulated amount of calcite.

Added amount of SO1	*n*, Adjustment index	Maximum accumulated amount of calcite (M)
1.0 g	3.2	6.26
0.1 g	3.2	5.58
0.01 g	3.2	4.85

Table 5

Modified parameters on the re-injection day of sequential analysis.

Re-injection day	Biomass of Re-injection day (mg/kg)	Maximum accumulation of calcite after re-injection day (M)
after 4 days	11331.25	6.68
after 7 days	10772.99	6.65
after 10 days	9193.96	6.55

Table 6

Precipitation amount of calcite in reproducible analysis.

Re-injection day	Simulated calcite precipitation (M)
after 4 days	8.01
after 7 days	7.97
after 10 days	7.82